Effects and mechanism of graphene-structured biochar on maize growth and soil amelioration: A case study in the Loess Plateau

Bowen Li[1], Xingyang Lai[2], Xiaofei Mao[3], Yang Xiong[1], Gang Li[2*], Nan Zhao[3,4*], Bo Xie[4,5]

(1. *College of Chemical Engineering, Huaqiao University, Xiamen 361021, Fujian, China*;
2. *School of Computer and Artificial Intelligence, Beijing Technology and Business University, Beijing 100048, China*;
3. *School of Ecology and Environment, Zhengzhou University, Zhengzhou 450001, China*;
4. *State Key Laboratory of Efficient Utilization of Medium and Low Grade Phosphate Rock and Its Associated Resources, Guiyang 550014, China*;
5. *Wengfu (Group) Co., Ltd, Guiyang 550001, China*)

Abstract: Land improvement technology effectively addresses the challenges of arable land shortages, soil degradation, and the food crisis. Graphene-structured biochar (G-biochar) emerges as a promising soil conditioner among the innovative solutions due to its unique properties and lower cost. This study conducted field experiments to monitor and evaluate soil quality recovery at various maize growth stages in loess. The results indicate that the lamellar structure of G-biochar enhances soil aggregation, reduces water evaporation, and increases soil moisture content by 17.6% compared to the control. Due to the interactions with cations through delocalized π electrons, G-biochar leads to the enrichment of nitrogen cations and adsorption of phosphate, specifically, the concentration of nitrate nitrogen and available phosphorus improved by 25.0% and 178%, respectively. The maize treated with G-biochar has a higher yield, nutrition, and germination rate. Additionally, G-biochar demonstrates remarkable performance in altering the abundance and composition of soil microbial communities. G-biochar significantly improves soil moisture content, quality, nutrient utilization, and modulates the soil microbiome in the test Loess Plateau, it may be used as a promising soil conditioner. This research provides a case analysis of G-biochar's impact on the maize-loess system. It explores the mechanisms underlying its function as a soil conditioner, offering theoretical support for its application in land improvement strategies.

Keywords: graphene-structured biochar, maize-loess system, nutrient utilization, microbial communities, soil moisture retention

DOI: 10.25165/j.ijabe.20261904.10537

Citation: Li B W, Lai X Y, Mao X F, Xiong Y, Li G, Zhao N, et al. Effects and mechanism of graphene-structured biochar on maize growth and soil amelioration: A case study in the Loess Plateau. Int J Agric & Biol Eng, 2026; 19(4): 143–151.

1 Introduction

Farmland plays a crucial role in ensuring food security and contributing to national prosperity[1]. However, agriculture faces numerous challenges due to its substantial resource demands, including a shortage of cultivated land, soil degradation, and an ongoing food crisis[2]. A report highlights a concerning trend in China, where the total area of arable land has diminished from 130 million hm² in 1995 to 127.5 million hm² in 2022[3]. To address these challenges and safeguard national food security, it is imperative to enhance the efficiency and productivity of land use, thereby supporting the sustainable development of agriculture. Currently, land improvement technology primarily relies on the application of both natural and artificial soil amendments, such as cellulose and polyacrylonitrile, to enhance soil particle formation and improve soil structure[4,5]. Additionally, alkaline substances like lime, sodium carbonate, and saltpeter ash are utilized to neutralize soil acidity[6]. Among these amendments, carbon materials have emerged as having significant potential for soil improvement due to their exceptional mechanical properties, electrical conductivity, and energy storage capabilities[7].

Biochar, for instance, is known to enhance soil quality by boosting microbial and enzyme activity, increasing soil organic carbon content, and improving the retention and availability of nutrients[8]. Similarly, carbon nanotubes contribute to water retention, temperature regulation, and nutrient supply[9]. Despite these promising applications, the production and processing of carbon materials remain complex and require advanced technology and costly equipment[10]. Furthermore, the effects and mechanisms of carbon materials on soil are not yet fully understood, necessitating comprehensive and systematic safety evaluations and monitoring. To achieve the desired effects in soil treatment, it is crucial to select and optimize the appropriate carbon material based on the specific characteristics of different soils. Graphene, a notable carbon material, is widely utilized in land improvement and soil remediation due to its exceptional properties, including excellent thermal and electrical conductivity, a high specific surface area, and adjustable porosity[11-13]. The high specific surface area and pore

Received date: 2026-02-27 **Accepted date:** 2026-07-14

Biographies: Bowen Li, PhD, research interest: resource utilization of waste, Email: libowen@hqu.edu.cn; **Xingyang Lai**, MS, research interest: resource utilization of waste, Email: laixingyang1226@163.com; **Xiaofei Mao**, MS, research interest: resource utilization of waste, Email: mao0127@gs.zzu.edu.cn; **Yang Xiong**, BS candidate, research interest: resource utilization of waste, Email: 2326311029@stu.hqu.edu.cn; **Bo Xie**, PhD, research interest: resource utilization of waste, Email: 1661958228@qq.com.

***Corresponding author: Gang Li**, Professor, PhD, research interest: Resource utilization of waste. School of Computer and Artificial Intelligence, Beijing Technology and Business University, Beijing 100048, China. Tel: +86-13401047576, Email: ligang@btbu.edu.cn; **Nan Zhao**, Professor, PhD, research interest: resource utilization of waste. School of Computer and Artificial Intelligence, Beijing Technology and Business University, Beijing 100048, China. Tel: +86-13838315063, Email: zhaonan@zzu.edu.cn.

structure of graphene enhance soil adsorption capacity, thereby reducing water loss and evaporation when used as a soil conditioner[14,15]. Furthermore, these properties provide numerous active sites for the effective absorption and fixation of pollutants, such as heavy metals, organic pollutants, and pathogens, making graphene an effective soil remediation agent[16]. Additionally, graphene's good electrical conductivity facilitates its participation in electrochemical reactions within the soil, aiding in the degradation or transformation of contaminants[17]. This conductivity also promotes electron transfer, thereby improving the redox conditions of the soil.

Graphene and its derivatives have been shown to influence the elemental composition of soil, playing a significant role in regulating maize growth[18]. Graphene oxide (GO), for instance, has the dual capability of preventing soil water evaporation and maintaining soil pH levels[19]. Despite these promising properties, the high cost of pristine graphene restricts its large-scale application in soil improvement. Furthermore, existing field studies on graphene-based amendments have been predominantly conducted in plain regions, with scant attention paid to the Loess Plateau, an ecologically vulnerable area prone to severe erosion and nutrient deficiency. This study developed a cost-effective graphene-structured biochar (G-biochar) and conducted a field experiment in a representative maize-loess system. Specifically, this study aimed to evaluate the effects of G-biochar on key soil physicochemical properties, assess the subsequent impacts on maize agronomic performance, and elucidate the underlying mechanisms of G-biochar action, with a focus on its modulation of rhizosphere microbial community structure and composition. By addressing these objectives, a comprehensive scientific basis was provided for the application of G-biochar as a low-cost and effective soil conditioner in degraded loess regions.

2 Materials and methods

2.1 G-biochar and soil

G-biochar, supplied by Changzhou 2D Carbon Technology Co., Ltd., plays a crucial role in this project. The G-biochar was made by lignin, and the flash Joule heat device was operated with a pulse voltage of 190 V and a pulse duration of 2500 ms. An electrical pulse was then discharged through the powders, causing the sample to reach ~3000 K rapidly. A prominent two-dimensional (2D) Raman peak was observed at approximately 2707 cm^{-1} in the Raman spectrum of G-biochar synthesized at 190 V, with an I_2D/I_G intensity ratio of 0.67, consistent with the characteristic spectral signature of graphene-like carbon materials (Figure 1). The surface area of G-biochar was measured to be 411 m^2/g, and the average pore diameter was 16.9 nm, significantly higher than that of typical biochar[20]. The project site is situated in Ma Town, Fugu County, Shaanxi Province (111.056 984°E, 39.374 374°N), within the Loess Plateau's hinterland and the Yellow River's earth and stone mountains. This area is characterized by its arid and semi-arid climate, which, combined with complex natural geographical conditions, contributes to significant challenges such as severe soil erosion, low fertility, and declining soil quality. The farmland in this region is predominantly abandoned, re-cultivated, or altered from slopes, and is largely scattered. These factors collectively underscore the need for innovative solutions to address the poor performance of the soil, exacerbated by windy sand and soil conditions.

2.2 Experimental design

The G-biochar was uniformly applied to the abandoned land. The soil was then leveled and plowed in accordance with standard management practices. At the surface layer, amendments and soil were thoroughly mixed through plowing, with the application rate calculated per hectare. On average, 0.56 t of G-biochar was required per hectare. Unified field management practices, such as land irrigation, mechanical sowing, fertilizer application, weed removal, and other conventional field operations, were implemented on both improved and unimproved farmland by an agricultural investment company. The experimental group, which incorporated graphene, was designated as the T group, while the control group, devoid of graphene, was referred to as the CK group.

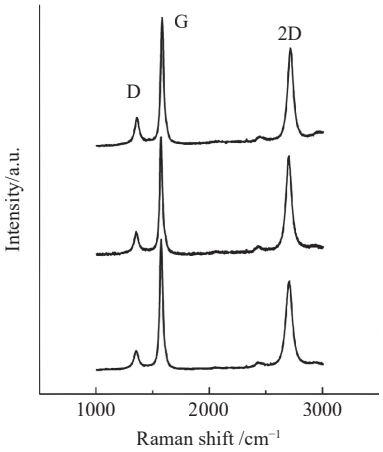


Figure 1 Raman spectrum of G-biochar

2.3 Sample collection

Prior to the application of G-biochar, a comprehensive soil quality survey was conducted to gather soil samples from the cultivated layer. In each plot, three blocks measuring 10 m×10 m were randomly selected. A five-point sampling method was employed within these areas, with soil samples collected from a depth of 0-20 cm using drills. The collected soil samples were then sealed and stored in the laboratory for further analysis. Initially, the soil was sieved through a 2 mm diameter mesh to remove impurities such as animal residues, small pebbles, plant twigs, and weeds. Approximately one-third of the soil was set aside for air drying, which facilitated the determination of its physical and chemical characteristics. The remaining soil samples were allocated for DNA sequencing to analyze microbial species. Furthermore, additional soil quality surveys were conducted during the maize growth period and after harvest, utilizing the same sample collection method as previously described.

At the maturity stage of maize, ten neighboring maize plants were selected from each plot for measurement of plant height. Following this, the maize samples were collected and divided into stover and grain portions. The weights of these portions were recorded, and the yield was calculated based on the sampled area. Subsequently, all the stalks and grains were thoroughly washed with tap water followed by ultrapure water. The samples were then dried at a temperature of 60°C-65°C until a constant weight was achieved. Then the samples were crushed using a stainless steel grinder and stored for further analysis.

Fresh roots were collected at the maize maturity stage from three randomly selected plants per plot. Root samples were gently rinsed with sterile phosphate-buffered saline to remove loosely attached soil particles, then fixed in 2.5% glutaraldehyde for 4 h at 4°C, followed by dehydration through a graded ethanol series (30%, 50%, 70%, 90%, and 100%). The samples were stored for further analysis.

2.4 Quality determination of soil and plant

The moisture content of the samples was determined using the drying method. Organic carbon content was assessed using the potassium dichromate capacity method. The total nitrogen (TN), total phosphorus (TP), and total potassium (TK) contents were analyzed after digestion with a microwave digestion instrument (MARS6, CEM Corporation, USA) through Kjeldahl nitrogen determination, vanadium-molybdenum yellow colorimetric method, and flame photometer method, respectively. Ammonium and nitrate concentrations in the samples were extracted with 0.5 mol/L K_2SO_4 and determined by the indophenol blue method and the vanadium oxidation method[21]. Available phosphorus was extracted using 0.5 mol/L $NaHCO_3$ (Olsen method) and quantified by the vanadium-molybdenum yellow colorimetric method. The total protein content of maize grain was determined by Kjeldahl method, while the total fat content was measured using Soxhlet extraction. The concentration of total starch content, total cellulose, total dietary fiber, insoluble dietary fiber, and soluble dietary fiber were determined according to the method proposed by Lv et al.[22] The composition and content of fatty acids were analyzed using gas chromatography-mass spectrometry (GC-MS, 7890, Agilent Technologies, USA). Additionally, the microstructure of maize roots was examined using a scanning electron microscope (GeminiSEM 300, Germany).

2.5 DNA extraction, PCR amplification, and Illumina MiSeq analysis of soil microbial communities

Microbial DNA was extracted from 0.5 g of stored soil samples using a Soil DNA Kit (Mobio Laboratories, Carlsbad, CA, USA) following the manufacturer's protocols. The extracted DNA was then assessed for quality by running it on a 1% agarose gel, and its concentration and purity were measured using a NanoDrop 2000 UV-vis spectrophotometer (Thermo Scientific, Wilmington, USA). All DNA samples were subsequently stored at –80°C to preserve their integrity. For the amplification of the hypervariable region V3-V4 of the bacterial 16S rRNA gene and the fungal ITS gene, primer pairs 515F and 806R, as well as ITS1 and ITS2, were employed, respectively. The PCR amplification process followed the methodology described by Li et al.[23] Post-amplification, the PCR products were extracted from a 2% agarose gel and purified using the AxyPrep DNA Gel Extraction Kit (Axygen Biosciences, Union City, CA, USA) according to the manufacturer's instructions.

The purified DNA was quantified using a Quantus™ Fluorometer (Promega, USA). Subsequently, the purified amplicons were pooled in equimolar concentrations and subjected to paired-end sequencing on an Illumina MiSeq PE300 platform (Illumina, San Diego, USA), adhering to the standard protocols provided by Majorbio Bio-Pharm Technology Co. Ltd. (Shanghai, China).

2.6 Scanning electron microscope (SEM)

The specimens were gold-coated and examined using a scanning electron microscope (GeminiSEM 300, Germany) at 50, 100, 500, and 1000 times magnifications by using an acceleration voltage of 3 kV. Biofilm coverage was qualitatively assessed by visually comparing SEM images from CK and T groups.

2.7 Statistical analysis

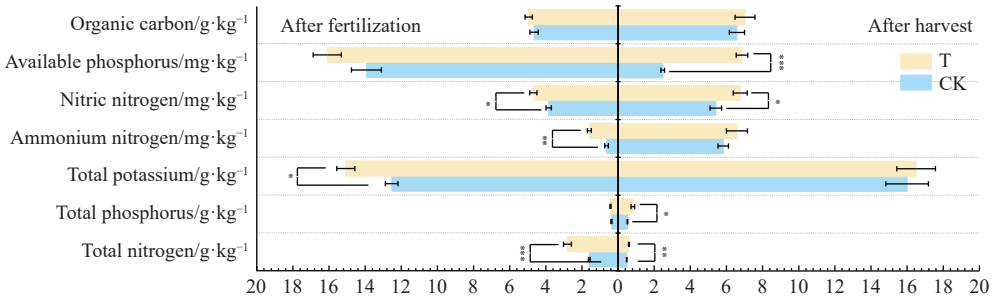
Mapping and data analysis were conducted using Origin2021 (Original Laboratory, Northampton, USA) and SPSS 19.0 (IBM Corporation, Armonk, USA) software. Prior to statistical analysis, the data underwent assessments for normality and homogeneity of variance. In cases where the data did not follow a normal distribution, non-parametric tests were employed. All results are presented as mean values with their corresponding standard errors. Additionally, microbial analysis was performed using the Majorbio Cloud platform (Majorbio Bio-Pharm Technology Co. Ltd.).

3 Results and discussion

3.1 Effect of G-biochar application on soil quality

The results of the study demonstrate that the application of graphene significantly enhances soil water retention capacity. Specifically, the soil moisture content increased from 7.24%±0.17% in the control group to 8.51%±0.23% in the treatment group, representing a 17.6% improvement with G-biochar treatment. Loess soil, being loose and porous, is prone to water loss. However, the lamellar structure of G-biochar increases soil density, effectively reducing the evaporation and escape of water molecules, thereby maintaining soil moisture content and providing adequate water for maize growth.

In addition to improving water retention, G-biochar also enhances soil fertility by increasing nutrient concentrations. Before G-biochar application, baseline soil properties were comparable between the CK and T plots (0.55-0.65 g/kg). After the incorporation of G-biochar and base fertilizer, soil samples were collected immediately before sowing. At this stage, the T group exhibited significantly higher levels of TN, TK, ammonium nitrogen (NH_4^+-N), and nitrate nitrogen (NO_3^--N) than the CK group, with values of 2.80±0.22 g/kg, 15.07±0.50 g/kg, 1.59±0.11 mg/kg, and 4.69±0.20 mg/kg, respectively, compared to 1.59±0.05 g/kg, 12.53±0.35 g/kg, 0.64±0.10 mg/kg, and 3.84±0.15 mg/kg in the CK group (Figure 2).



Note: *Significantly different at the 0.05 probability level; **Significantly different at the 0.01 probability level; ***Significantly different at the 0.001 probability level. The same as below.

Figure 2 Nutrient concentration of the soil after fertilization and harvest in CK and T group

After a maize growing season of approximately four months (120 d), the soil moisture content in the T group increased by 17.6% compared to the CK group. This increase in moisture was accompanied by significant enhancements in soil nutrients: total nitrogen, total phosphorus, and total potassium levels rose by 25.60%, 58.80%, and 2.93%, respectively. Notably, the levels of

ammonium nitrogen, nitrate nitrogen, available phosphorus, and total organic carbon improved by 13.20%, 25.00%, 178.00%, and 6.76%, respectively (Figure 2). The substantial increases in nitrate nitrogen and available phosphorus, which are readily available fertilizers for plants, were particularly noteworthy. In the CK group, nitrate nitrogen and available phosphorus levels were 5.41±0.32 and 2.47±0.10, respectively, whereas in the T group, these levels rose to 6.76±0.29 and 6.86±0.32, indicating a significant enhancement.

The results of G-biochar application on soil quality suggest that G-biochar possesses excellent capabilities for retaining soil fertilizer. The soil treated by G-biochar provides sufficient nitrogen to support plant and microorganism growth[3]. G-biochar possesses a large specific surface area (411 m^2/g) and abundant delocalized π electrons on its graphene-like basal planes. These features enable strong cation-π interactions with ammonium (NH_4^+), leading to its surface enrichment and reduced leaching[24,25]. This is consistent with the observed 13.2% increase in NH_4^+-N. However, nitrate (NO_3^-) is an anion and does not directly bind to π electrons. The observed 25.0% increase in NO_3^--N is more likely indirect, perhaps resulting from G-biochar's improvement of soil aeration and water retention, which may enhance nitrification by aerobic ammonia-oxidizing microorganisms. Additionally, the retention of NH_4^+ provides a larger substrate pool for subsequent nitrification. These possibilities warrant further investigation.

Adequate phosphate availability promotes vigorous root and above-ground growth, facilitates biochemical cycling, and improves water-use efficiency[3]. The remarkable increase in available P can be attributed to multiple factors. The alkaline nature of loess soil (pH ~8.2) typically limits P availability due to Ca-P precipitation. However, G-biochar addition may locally lower pH or provide organic ligands that compete with phosphate for Ca^{2+} binding sites, thereby releasing occluded P. Meanwhile, G-biochar could directly adsorb and then slowly release phosphate, acting as a P reservoir. Further studies are needed to partition these contributions.

3.2 Effect of G-biochar application on maize growth

The study's findings indicate that G-biochar significantly enhances various stages of maize growth. During the germination stage, maize in the treatment group germinated 1-3 d earlier than the control group, with an increase in seedling emergence rate by 10%-30%. Furthermore, maize seedlings treated with G-biochar exhibited enhanced robustness, demonstrating strong resistance to late frosts, improved fiber quality in later stages, and a high degree of lignification. The dark color of G-biochar absorbs more energy, raising soil temperature and further promoting plant germination and growth within the maize-loess system. G-biochar significantly enhances various stages of maize growth. Due to its dark black color, G-biochar particles can absorb solar heat energy, leading to an increase in soil temperature. This rise in temperature is particularly beneficial in breaking the dormancy of maize seeds, thereby accelerating germination and improving the rate of seedling emergence[26]. These effects are especially pronounced in soils with lower fertility and arid conditions. Additionally, graphene facilitates water absorption by penetrating the seed shell, further aiding in seed germination[27].

During the elongation stage of maize growth, significant differences were observed between the CK group and the T group. In the CK group, maize height ranged from 42 to 70 cm, whereas in the T group, it ranged from 90 to 110 cm. Additionally, the number of emerged plants per 9 m^2 was 41-44 in the CK group, compared to 47-50 in the T group. The application of G-biochar treatment resulted in increased seedling emergence, taller and more uniformly emerged maize plants, as well as wider leaves and more vigorous growth. Notably, the water content in the T group was significantly higher than in the CK group, with a 47.9% increase in the rhizosphere water content. This enhancement in water retention can be attributed to G-biochar's large specific surface area, which effectively adsorbs water in the soil. In Fugu County, where the soil is characterized by a high sand content and softness, G-biochar plays a crucial role in reducing water evaporation from the soil surface, preventing water seepage, and maintaining soil moisture.

In the maturity stage of maize, significant improvements were observed in plants grown in G-biochar treated soil compared to the CK group. Maize stalks from the G-biochar treatment were notably taller, coarser, and brighter in color. Specifically, the fresh weight, dry weight, moisture content, and height of these stalks were 111%, 78.6%, 9.70%, and 15.4% higher, respectively, than those in the CK group. Additionally, the maize root system in the T group exhibited an increase in fresh weight of 139% ($p<0.05$) and in moisture content of 22.1% ($p<0.001$) compared to the CK group. Although the root dry weight showed an apparent increase of 50.0%, this difference did not reach statistical significance ($p=0.178$; Table 1), possibly due to biological variation among replicates. Nevertheless, the substantial increase in root fresh weight and moisture content suggests that G-biochar primarily enhanced root water uptake capacity, which may indirectly contribute to the observed trends in biomass accumulation. This is consistent with the observed 22.1% increase in root moisture content (Table 1) and the improved rhizosphere water availability noted in section 3.1.

Table 1 Weight and c content of maize stalks and roots at the maturity stage

Maize	Group	Fresh weight/g	Dry weight/g	Moisture content/%	Height/m
Stalk	CK	375.3±64.3	148.0±21.7	60.0±3.2	2.20±0.04
	T	791.0±84.1	264.7±21.3	65.7±5.2	2.57±0.01
p-value		0.017*	0.018*	0.407	0.001**
Root	CK	203.0±34.4	76.3±13.9	61.1±0.8	-
	T	484.7±61.3	113.7±18.2	76.2±1.0	-
p-value		0.016*	0.178	0.0003***	-
Grain	CK	280.7±51.0	183.7±34.3	34.7±1.1	-
	T	478.0±29.2	248.3±34.6	48.6±4.1	-
p-value		0.028*	0.255	0.030*	-

*Significantly different at the 0.05 probability level; **Significantly different at the 0.01 probability level; ***Significantly different at the 0.001 probability level. The same as below.

Although G-biochar particles may interact with the root surface and potentially endocytosis at the root hair apex to enter the outermost cell layers[28], direct evidence for such internalization in the present maize-loess system is unavailable. Nevertheless, the observed acceleration of root growth and cell division in the root end meristematic tissue is likely mediated by G-biochar-induced improvements in rhizosphere water and nutrient availability rather than by direct physical penetration of graphene nanostructures into root cells.

3.3 Effect of G-biochar application on plant and grain nutrition

The application of G-biochar has significantly enhanced the nutrient and water supply in previously abandoned land, thereby promoting the growth of maize. This improvement is evident in the increased content of total nitrogen, total phosphorus, and total potassium in maize stalks. Specifically, in the CK group, the TN, TP, and TK contents were 2.06±0.03, 0.20±0.01, and 10.13±0.84, respectively. In contrast, the T group exhibited higher values of

3.04±0.10 for TN, 0.24±0.01 for TP, and 14.37±0.93 for TK. This represents an increase of 47.81%, 20.34%, and 41.78% in TN, TP, and TK content, respectively, with the application of G-biochar (Figure 3). The enhanced nutrient availability stimulates maize growth, resulting in more robust aboveground vegetative structures. This growth is reflected in increased plant height, stem thickness, and number of leaves, maize ears, and grains, ultimately providing more nutrients for the maize.

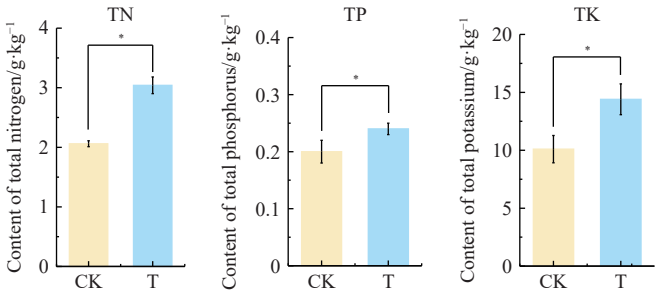


Figure 3 TN, TP, and TK content of maize stalk in CK and T group

In comparison to the CK group, the maize grains harvested in the T group exhibited enhanced fullness and nutritional value. Specifically, the total protein, total fat, total starch, total cellulose, and total dietary fiber content increased by 8.66%, 4.48%, 0.69%, 12.70%, and 5.90%, respectively. Additionally, the insoluble and soluble dietary fiber contents rose by 5.80% and 1.94%, respectively (Figure 4). The content of unsaturated fatty acids, including methyl myristate, methyl palmitate, methyl cis-10-heptadecenoate, methyl heptadecanoate, methyl linoleate, elaidic acid methyl ester, methyl oleate, methyl cis-11-eicosenoate, methyl docosanoate, and methyl tetracosanoate, increased by 69.4%, 18.1%, 8.40%, 10.0%, 10.9%, 7.23%, 11.7%, 32.5%, 5.07%, 29.0%, and 5.66%, respectively (Table 2). The maize grain's protein, total fiber, and unsaturated fatty acid content (using linoleate methyl ester as an example) increased by 4.2 g/kg, 3.6 g/kg, and 522 mg/kg, respectively. When calculated based on the edible portion of maize being 80%, the nutritional value per hectare increased by 250 kg for protein, 29 kg for fiber, and 35 kg for unsaturated fatty acids. The moderate increases in total protein (+8.66%) and fat (+4.48%), coupled with the negligible change in total starch (+0.69%, $p>0.05$), suggest a shift in carbon allocation toward nitrogen- and lipid-rich storage compounds under G-biochar treatment. This pattern may be attributed to G-biochar-enhanced nitrogen availability, which preferentially supports protein synthesis, as well as potential changes in starch metabolism gene expression induced by graphene exposure. This pattern aligns with observations in other biochar-amended cropping systems, where biochar application often increased grain protein and oil content while causing variable effects on starch[29].

3.4 Response of soil microbial communities to G-biochar application

The diversity of soil microorganisms plays a crucial role in maintaining the functionality of plant-soil systems[30,31]. In this study, a comparison of bacterial species richness between the CK and T groups revealed significant differences at the genus level, as indicated by the ace index and confirmed by a Student's t-test ($p<0.05$). The coverage index for each group exceeded 0.97, indicating that the test results accurately reflect the actual conditions of the samples.

Figure 5 illustrates the composition of the microbial community at the phylum level in both the CK and T groups. The results reveal that the soil microorganisms predominantly comprise *Actinobacteriota*, *Proteobacteria*, *Bacteroidota*, *Chloroflexi*, *Ascomycota*, and *Chytridiomycota*, among others. Especially, the microbial community structure underwent significant changes following treatment with G-biochar. A comparative analysis of the phylum-level differences between the two groups shows that the abundance of *Bacteroidota*, *Chloroflexi*, *Myxococcota*, and *Basidiomycota* was significantly higher in the CK group than in the T group. Conversely, the abundance of *Cyanobacteria*, *Deinococcota*, *GAL15*, *Methylomirabilota*, *Planctomycetota*, and *Chytridiomycota* was considerably greater in the T group ($p<0.05$). The enhanced water retention capacity of G-biochar increases the soil's moisture content, thereby promoting the growth of *Cyanobacteria* and *Chytridiomycota*, which thrive in humid environments. Additionally, the observed increase in *Deinococcota* is more likely attributable to indirect ecological shifts within the soil microbial community.

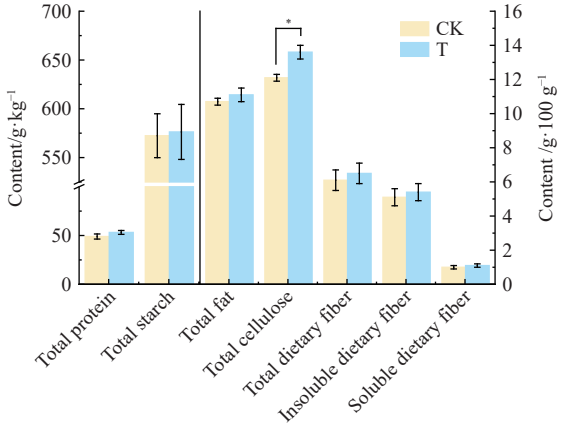


Figure 4 Nutrient composition of maize grain in CK and T group

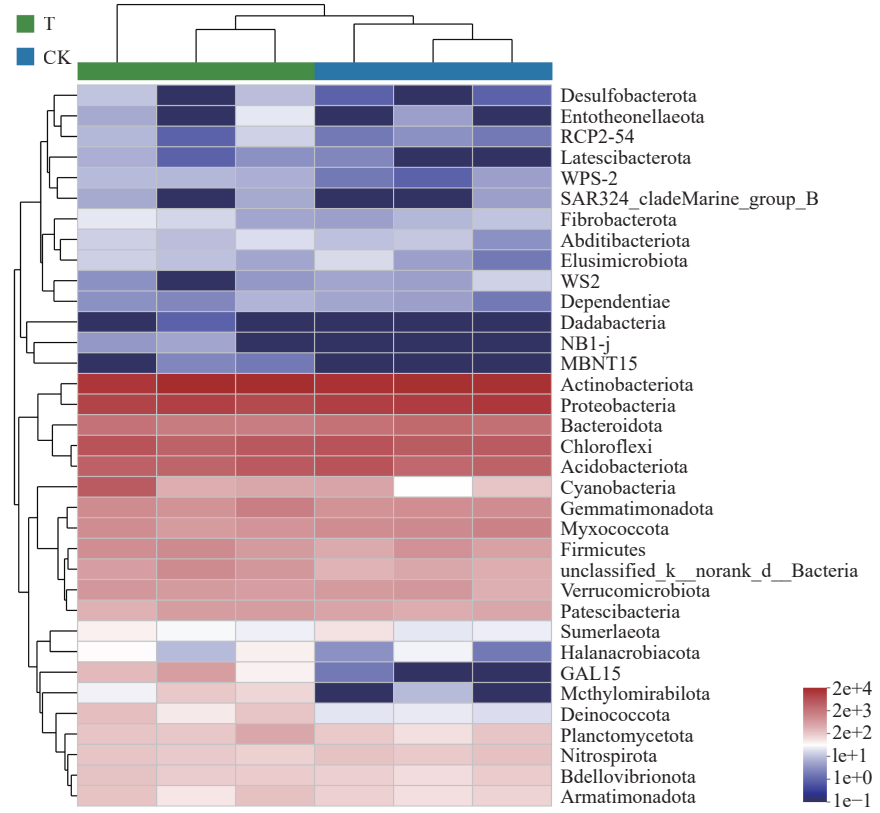
Table 2 Fatty acids composition of maize grain in CK and T group

Index	CK	T	*p*-value
Methyl myristate/mg·kg⁻¹	7.9±0.3	13.4±0.02	0.0003***
Methyl palmitoleate/mg·kg⁻¹	23.6±5.1	27.9±2.9	0.508
Methyl palmitate/mg·kg⁻¹	2509.2±350.7	2719.9±98.0	0.594
Methyl cis-10-heptadecenoate/mg·kg⁻¹	19.9±2.5	21.8±1.4	0.522
Methyl heptadecanoate/mg·kg⁻¹	4.8±1.5	5.4±1.5	0.819
Methyl linoleate/mg·kg⁻¹	7215.4±844.3	7736.8±312.3	0.594
Elaidic acid methyl ester/mg·kg⁻¹	1015.6±71.5	1134.1±97.9	0.384
Methyl oleate/mg·kg⁻¹	269.3±16.8	356.8±9.5	0.011*
Methyl stearate/mg·kg⁻¹	425.2±122.7	390.0±44.1	0.800
Methyl cis-11-eicosenoate/mg·kg⁻¹	28.7±10.9	30.1±2.1	0.902
Methyl arachidate/mg·kg⁻¹	67.3±27.2	66.4±7.6	0.976
Methyl docosanoate/mg·kg⁻¹	15.3±3.1	19.7±8.8	0.661
Methyl tetracosanoate/mg·kg⁻¹	72.5±8.5	76.6±3.4	0.677

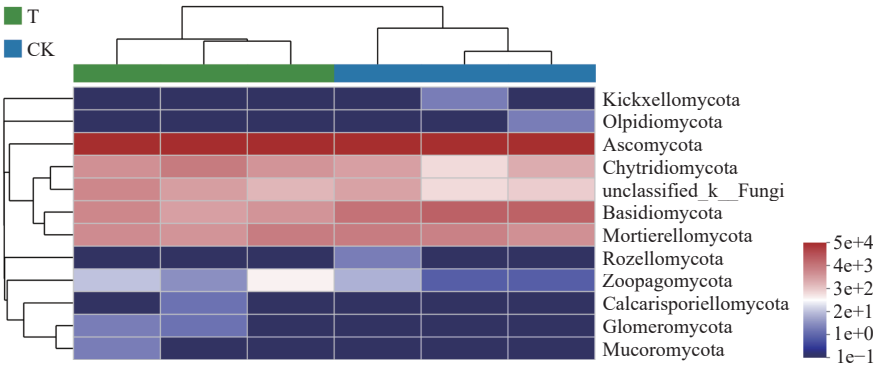
The analysis of microbial communities in soil samples from the CK and T groups revealed no significant differences in the overall abundance of *Actinobacteriota*, *Proteobacteria*, and *Ascomycota*, which were the most abundant phyla. However, a more detailed examination indicated significant compositional differences between the two groups in *Acidobacteriota*, *Actinobacteriota*, *Proteobacteria*, and *Ascomycota*. Lefse analysis provided insights into the microbial community composition from the phylum to the genus level (Figure 6). Notably, *Xanthomonadales*, a member of

Proteobacteria known for containing numerous phytopathogenic bacteria, were more prevalent in the CK group than in the T group. In contrast, *Metarhizium*, an *Ascomycota* fungus known for its ability to infect maize pests, was significantly more abundant in the T group than in the CK group. Additionally, the order *Spizellomycetalean*, part of the *Chytridiomycetes* class and known for its beneficial roles in nutrient recycling and parasitism of plant-attacking organisms, was found in higher abundance in the T group. The higher abundance of *Cyanobacteria* in the T group is consistent with the known ecology of these microorganisms, which form biological crusts in response to increased surface moisture[32]. Similarly, the enrichment of *Chytridiomycota* is ecologically plausible, as their zoosporic reproduction requires free water[33].

SEM observation of the root surface revealed a substantial reduction in bacterial biofilm coverage in the T group compared to the CK group (Figure 7). This qualitative observation suggests that G-biochar may help mitigate the risk of bacterial root infections, although quantitative assessments (e.g., crystal violet staining or colony-forming unit counts) are needed to confirm this effect. The observed reduction in biofilm formation could be attributed to the combined effects of improved root health and potential antimicrobial properties of G-biochar.



a. Bacteria at the phylum level

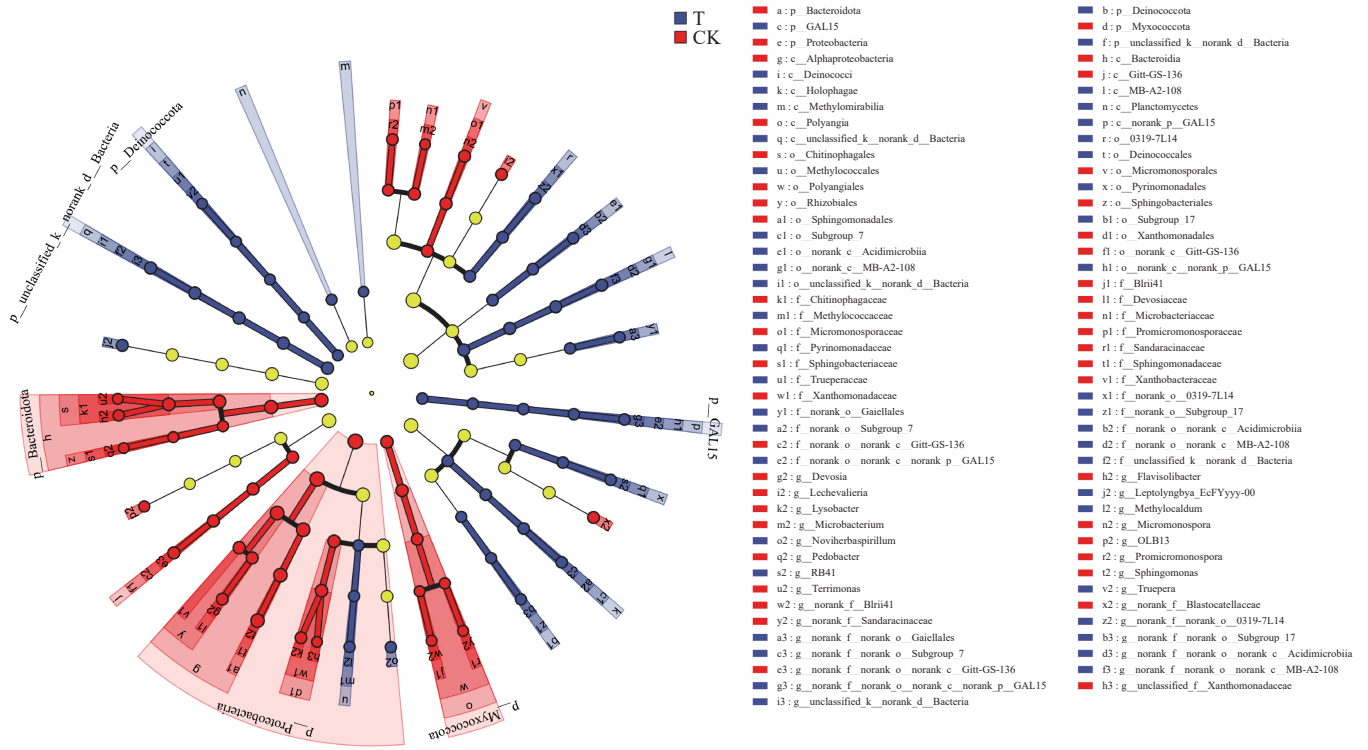


b. Fungi at the phylum level

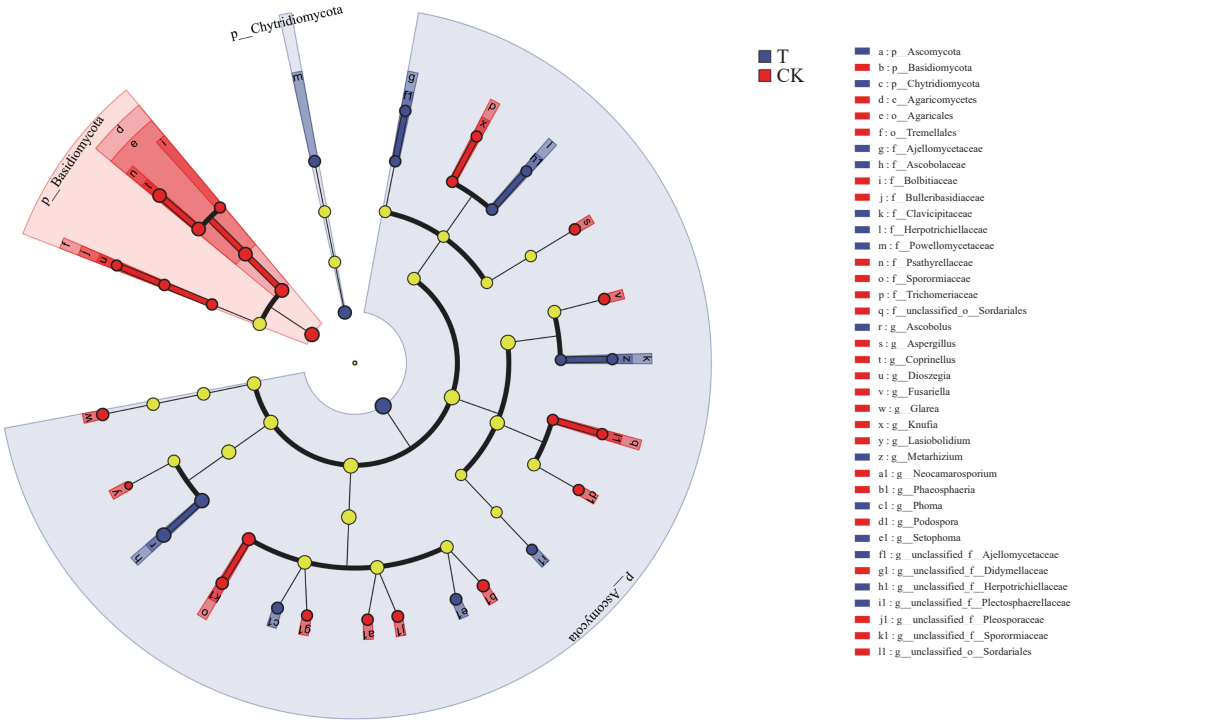
Figure 5 Heatmap analysis of microbial community in the CK and T group

Furthermore, the bacterial biofilm in the root system was significantly reduced in the T group compared to the CK group (Figure 7), effectively mitigating the risk of bacterial infectious diseases. These findings suggest that G-biochar has a potential role in plant disease prevention. The lamellar structure of G-biochar has been shown to exhibit antimicrobial activity, where nanoscale sharp edges can physically disrupt bacterial cell membranes[34,35]. It is plausible that a similar mechanism may contribute to the suppression of certain phytopathogenic bacteria in the present soil system. However, whether G-biochar particles retain their sharp-edge morphology and remain accessible to bacterial cells in the complex soil matrix, where they can be coated by organic matter or clay minerals, requires further validation. The observed reduction in pathogenic taxa such as *Xanthomonadales* may also result from indirect effects, including G-biochar-induced improvements in soil water and nutrient status that promote plant health and root

exudation patterns unfavorable for pathogen colonization. Thus, while the direct antimicrobial mechanism cannot be ruled out, the relative contributions of direct and indirect effects in modulating soil microbial communities remain to be quantified.



a. Bacteria



b. Fungi

Figure 6 Lefse analysis of microbial community in the CK and T group

3.5 Integrated mechanisms of G-biochar action and environmental considerations

The application of G-biochar in loess soil has been shown to positively influence maize growth, as previously discussed. Specifically, G-biochar amendment accelerates seed germination and enhances vegetative development, evidenced by increased plant height, improved biomass accumulation, and elevated tissue concentrations of essential nutrients (e.g., nitrogen, phosphorus, and potassium). These physiological improvements are underpinned by G-biochar's multifaceted influence on key soil properties: notably, enhanced water retention capacity, augmented nutrient availability, and modulation of soil microbial community composition and function (Figure 8).

Loess soil is inherently characterized by low bulk density, high porosity, and poor water-holding capacity, factors that predispose it to rapid moisture loss via evaporation and percolation. G-biochar's

two-dimensional lamellar architecture increases soil particle cohesion and reduces interstitial pore space, thereby impeding water vapor diffusion and minimizing evaporative losses. Concurrently, G-biochar's high surface absorptivity, attributable to its dark color, enhances solar energy capture, leading to moderate increases in soil temperature. This thermal effect synergistically supports early-stage seed germination and root metabolic activity in maize.

As a two-dimensional carbon nanomaterial with exceptional electron delocalization and aromatic stability, G-biochar exhibits strong cation-binding affinity via π–cation interactions. This facilitates the surface enrichment and stabilization of bioavailable nitrogen cations, thereby improving cation exchange capacity and mitigating leaching losses. Furthermore, G-biochar-mediated complexation between phosphate anions and metal cations (e.g., Fe, Al, Ca) can modulate phosphorus speciation and bioavailability, influencing long-term nutrient cycling dynamics. Collectively, these physicochemical modifications establish a more favorable edaphic environment for both maize root development and beneficial rhizosphere microbiota.

In addition, G-biochar's atomically thin, edge-rich lamellar morphology confers intrinsic antimicrobial properties. Its nanoscale sharp edges can physically penetrate and disrupt the integrity of bacterial cell membranes. By selectively suppressing phytopathogenic microbes while preserving or promoting beneficial taxa (e.g., plant-growth-promoting rhizobacteria), G-biochar contributes to a more resilient and functionally balanced soil microbiome, ultimately reinforcing maize health and productivity.

While the present results demonstrate clear short-term benefits of G-biochar application on soil quality, maize productivity, and microbial community modulation, it is equally important to consider the potential environmental implications of introducing this carbon nanomaterial into agricultural soils. As with other engineered nanomaterials, G-biochar particles may persist in the soil matrix over extended periods, and their gradual accumulation could potentially pose risks to non-target soil organisms through physical interaction or oxidative stress pathways, as reported for certain graphene-based materials in controlled exposure systems[36]. Additionally, the long-term fate of G-biochar remains largely unknown, including its potential fragmentation, chemical transformation, or vertical migration into deeper soil layers and groundwater. In the current field trial, visual phytotoxicity symptoms in maize plants were not observed. Nevertheless, these preliminary observations do not constitute a comprehensive ecological risk assessment. Future studies should systematically evaluate the dose-dependent, chronic, and food-web-level effects of G-biochar, as well as its interactive behavior with co-occurring soil contaminants, to ensure its safe and sustainable application in land improvement strategies.

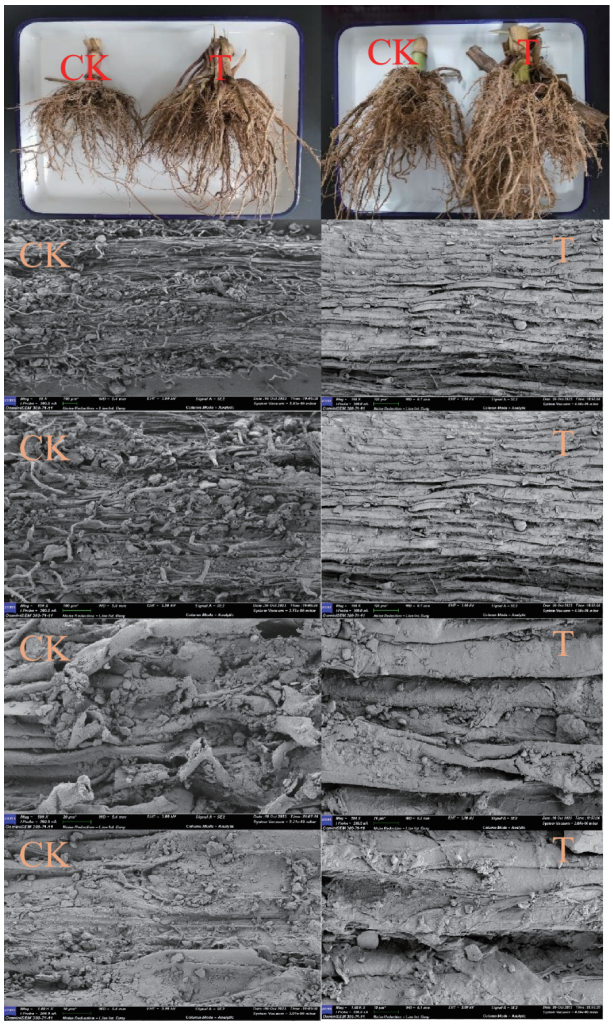


Figure 7 Macrostructure and microstructure of maize roots in CK and T group

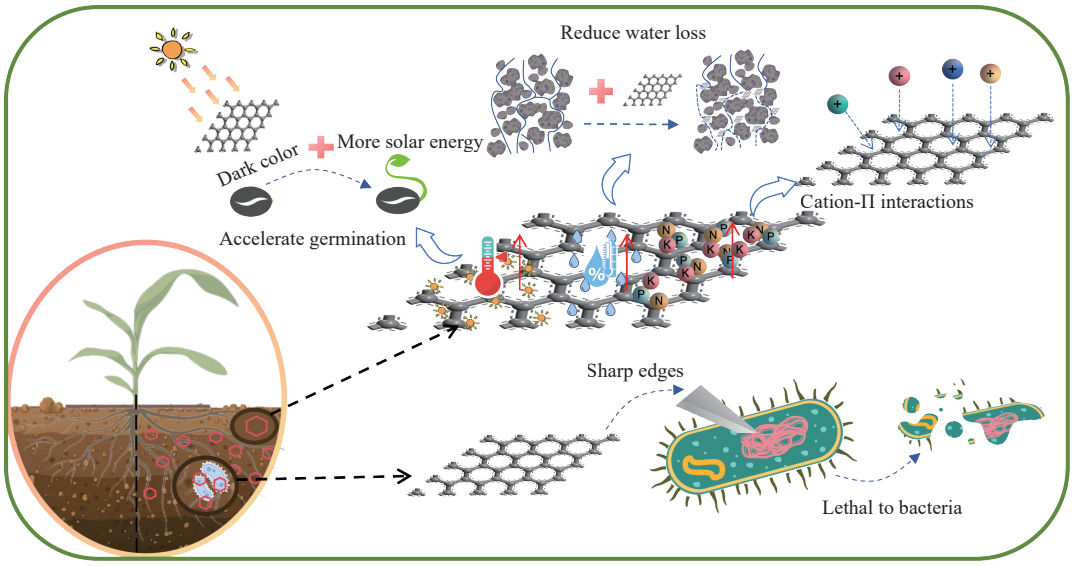


Figure 8 Behavior of G-biochar in the maize-loess soil system

4 Conclusions

This study examines the effects of G-biochar on maize growth, soil quality, and soil microorganisms within the maize soil system. The findings indicate that applying an appropriate amount of G-biochar to the soil enhances soil quality and structure while increasing the content of available nutrients and regulating the composition of the microbial community. Furthermore, G-biochar facilitates crop rooting and germination, leading to significant improvements in maize yield and fruit fullness. This research contributes to the understanding of the regulatory mechanisms of G-biochar in soil environments and its growth-promoting effects on crops. However, further investigation is needed to assess the long-term effects of G-biochar materials on the soil environment and explore the impact of G-biochar on other crops.

Acknowledgements

This work was supported by the National Natural Science Foundation of China (Grant No. 52200177; 52470164), the Natural Science Foundation of Xiamen Municipality (3502Z202471038), the Young Elite Scientist Sponsorship Program by CAST (YESS20230603), the Open Research Fund Program of the State Key Laboratory of Clean and Efficient Coal Utilization of Taiyuan University of Technology (Grant No. SKL2022004), and the Open Research Fund Program of the State Key Laboratory of Efficient Utilization for Low Grade Phosphate Rock and Its Associated Resources (WFKF (2023) 007). This work was also supported by the Key Laboratory of Development and Application of Rural Renewable Energy, Ministry of Agriculture, China, and 2D Carbon (Changzhou) Tech Inc., Ltd.

[References]

[1] Chen Y H, He X H, Gao J Q, Wang F M, Hou Y H, Cai Q, et al. Biochar assisted bioremediation of soils with combined contamination of petroleum hydrocarbons and heavy metals: A review. Appl. Soil Ecol., 2024; 204: 105720.

[2] Wang Y B, Hu X D, Yu S X, Wang Z, Zhao J S, Fang N F, et al. Soil conservation of sloping farmland in China: History, present, and future. Earth-Sci. Rev., 2024; 249: 104655.

[3] Baysal A, Saygin H, Ustabasi G S. Risks of graphene nanomaterial contamination in the soil: Evaluation of major ions. Environ. Monit. Assess., 2020; 192: 622.

[4] Li G, Shan Y Y, Nie W B, Sun Y, Su L J, Mu W Y, et al. Application of carboxymethyl cellulose sodium (CMCNa) in maize–wheat cropping system (MWCS) in coastal saline-alkali soil. Sci. Total Environ., 2024; 912: 169214.

[5] Qin C C, Abdalkarim S Y H, Zhou Y, Yu H Y, He X. Ultrahigh water-retention cellulose hydrogels as soil amendments for early seed germination under harsh conditions. J. Clean. Prod., 2022; 370: 133602.

[6] Yang X D, Feng Y S, Zhang X H, Sun M X, Qiao D, Li J, et al. Mineral soil conditioner requirement and ability to adjust soil acidity. Sci Rep., 2020; 10: 18207.

[7] Wang Q L, Feng X Y, Liu Y Y, Cui W Z, Sun Y H, Zhang S W, et al. Effects of microplastics and carbon nanotubes on soil geochemical properties and bacterial communities. J. Hazard. Mater., 2022; 433: 128826.

[8] Gong H B, Zhao L, Rui X, Hu J W, Zhu N W. A review of pristine and modified biochar immobilizing typical heavy metals in soil: Applications and challenges. J. Hazard. Mater., 2022; 432: 128668.

[9] Chen X F, Wang J C, You Y M, Wang R Y, Chu S H, Chi Y W, et al. When nanoparticle and microbes meet: The effect of multi-walled carbon nanotubes on microbial community and nutrient cycling in hyperaccumulator system. J. Hazard. Mater., 2022; 423: 126947.

[10] Titirici M, White R J, Brun N, Budarin V L, Su D S, Del Monte F, et al. Sustainable carbon materials. Chem. Soc. Rev., 2015; 44: 250–290.

[11] Geim A K. Graphene: status and prospects. Science, 2009; 324(5934): 1530–1534.

[12] He K, Chen G, Zeng G Q, Peng M, Huang Z Z, Shi J B, et al. Stability, transport and ecosystem effects of graphene in water and soil environments. Nanoscale, 2017; 9: 5370–5388.

[13] Ponzelli M, Koch K, Drewes J E, Radjenovic J, Vinardell S. The ambivalent role of graphene oxide in anaerobic digestion: A review. Bioresour. Technol., 2024; 414: 131663.

[14] Alessandrino L, Pavlakis C, Colombani N, Mastrocicco M, Aschonitis V. Effects of graphene on soil water-retention curve, van Genuchten parameters, and soil pore size distribution—A comparison with traditional soil conditioners. Water, 2023; 15: 1297.

[15] Zhao L Q, Yang S T, Yilihamu A, Wu D Y. Advances in the applications of graphene adsorbents: From water treatment to soil remediation. Rev. Inorg. Chem., 2019; 39: 47–76.

[16] Toussi A G, Einafshar E, Rafati S S. Potential of graphene nanoparticles for reducing cadmium toxicity and environmental contamination. J. Toxicol., 2026; 1: 7838711.

[17] Alessandrino L, Eusebi A L, Aschonitis V, Mastrocicco M, Colombani N. Variation of the hydraulic properties in sandy soils induced by the addition of graphene and classical soil improvers. J. Hydrol, 2022; 612: 128256.

[18] Chen Z, Li H, Ma W D, Fu D, Han K, Wang H T, et al. Addition of graphene sheets enhances reductive dissolution of arsenic and iron from arsenic contaminated soil. Land Degrad. Dev., 2018; 29: 572–584.

[19] Zhao D Q, Fang Z W, Tang Y H, Tao J. Graphene oxide as an effective soil water retention agent can confer drought stress tolerance to paeonia ostii without toxicity. Environ. Sci. Technol., 2020; 54: 8269–8279.

[20] Cui Y D, Chen X, Pitakrattanawong C, Du X L, Qiu L P, Xu H M, et al. Adsorption efficiency of biochar produced by aquaculture by-products for removing geosmin in aquaculture environment. Water Reuse, 2024; 14(1): 65–79.

[21] Jing Y L, Zhang Y H, Han I, Wang P, Mei Q W, Huang Y J. Effects of different straw biochars on soil organic carbon, nitrogen, available phosphorus, and enzyme activity in paddy soil. Sci Rep., 2020; 10: 8837.

[22] Lv J S, Liu X Y, Zhang X P, Wang L S. Chemical composition and functional characteristics of dietary fiber-rich powder obtained from core of maize straw. Food Chemistry, 2017; 227: 383–389.

[23] Li B W, Zhao N, Ran X L, Zheng Y H, Sobhi M, Dong R J, et al. The effect of slow-release phosphate fertilizers from digestates on maize rhizosphere soil microbial community and nutrient cycling: Response and activation mechanism. Appl. Soil Ecol., 2024; 201: 105528.

[24] Katsnelson M I. Graphene: Carbon in two dimensions. Mater. Today, 2007; 10: 20–27.

[25] Zhao G K, Zhu H W. Cation-pi interactions in graphene-containing systems for water treatment and beyond. Adv. Mater., 2020; 32: 1905756.

[26] Khaeim H, Kende Z, Jolánkai M, Kovács G P, Gyuricza C, Tarnawa Á. Impact of temperature and water on seed germination and seedling growth of maize (*Zea mays* L.). Agronomy-Basel, 2022; 12: 397.

[27] Zhang M, Gao B, Chen J J, Li Y C. Effects of graphene on seed germination and seedling growth. J. Nanopart. Res., 2015; 17: 8.

[28] Dong S P, Jing X P, Lin S J, Lu K, Li W F, Lu J J, et al. Root hair apex is the key site for symplastic delivery of graphene into plants. Environ. Sci. Technol., 2022; 56(17): 12179–12189.

[29] Laharia G S, Fandi V, Age A B, Jadhao S D, Jadhvar P R. Effect of biochar on yield, quality and uptake of nutrients by maize grown on a vertisol in Maharashtra. India J. Nat. Resour. Conserv. Manag., 2022; 3(2): 152–158.

[30] Nannipieri P, Ascher-Jenull J, Ceccherini T M, Landi L, Pietramellara G, Renella G. Microbial diversity and soil functions. Eur. J. Soil Sci., 2017; 68: 12–26.

[31] Furtak K, Gajda A M. Activity and variety of soil microorganisms depending on the diversity of the soil tillage system. In: De Oliveira A B, editor. Sustainability of Agroecosystems. 2018; pp.45–60. doi: 10.5772/intechopen.72966.

[32] Kozar D, Weber B, Zhang Y, Dong X L. Spatial signatures of biological soil crusts and community level self-organization in drylands. Ecosystems, 2024; 27(3): 443.

[33] Freeman K R, Martin A P, Karki D, Lynch R C, Mitter M S, Meyer A F, et al. Evidence that chytrids dominate fungal communities in high-elevation soils. Proc. Natl. Acad. Sci., 2009; 106(43): 18315–18320.

[34] Dallavalle M, Calvaresi M, Bottoni A, Melle-Franco M, Zerbetto F. Graphene can wreak havoc with cell membranes. ACS Appl. Mater. Interfaces, 2015; 7: 4406–4414.

[35] Zhou R H, Gao H J. Cytotoxicity of graphene: Recent advances and future perspective. Wiley Interdiscip. Rev. Nanomed. Nanobiotechnol., 2014; 6: 452–474.

[36] Zhao S L, Wang Y L, Duo L. Biochemical toxicity, lysosomal membrane stability and DNA damage induced by graphene oxide in earthworms. Environ. Pollut., 2021; 269: 116225.